RSC Advances

PAPER

View Article Online
View Journal | View Issue

Cite this: *RSC Adv.*, 2017, **7**, 18803

Stability behaviour of antiretroviral drugs and their combinations. 6: evidence of formation of potentially toxic degradation products of zidovudine under hydrolytic and photolytic conditions†

Moolchand Kurmi, Archana Sahu, Shobhit Kumar Tiwari and Saranjit Singh *

This study explored the comprehensive degradation behaviour of zidovudine (ZDV) under solution and solid stress conditions. In total, nine degradation products were detected by high performance liquid chromatography (HPLC). The same were tentatively characterized with the help of high resolution and multistage mass spectrometry. Among them, five degradation products were also enriched and isolated with the help of semi-preparative HPLC and subjected to 1D and 2D nuclear magnetic resonance and/or infrared spectrometric studies to confirm their structures. The characterization of all the degradation products helped in outlining the comprehensive degradation pathway of ZDV. A significant finding was the formation of 3′-amino-3′-deoxythymidine (AMT) upon base hydrolysis as well as photolysis of the drug. This product is a known catabolite of the drug with a high degree of toxicity. Also, a few other degradation products formed during the study were predicted to have potential toxicity.

Received 16th January 2017
Accepted 3rd March 2017

DOI: 10.1039/c7ra00678k

rsc.li/rsc-advances

Introduction

In this sixth part of the series of studies on stability behaviour of antiretroviral drugs and their combinations,[1–5] we re-examined the stress degradation behaviour of zidovudine (ZDV, formerly AZT, 1-[(2*R*,4*S*,5*S*)-4-azido-5-(hydroxymethyl)tetrahydrofuran-2-yl]-5-methylpyrimidine-2,4(1*H*,3*H*)-dione). The drug is a first nucleoside reverse transcriptase inhibitor, which was approved by the United States Food and Drug Administration (USFDA) in 1987 for the treatment of acquired immunodeficiency syndrome (AIDS).[6] In our previous reports,[7,8] we identified 5-methylpyrimidine-2,4(1*H*,3*H*)-dione (thymine) as the major degradation product of the drug under hydrolytic and photolytic conditions. In a recent paper, Devrukhakar *et al.*[9] identified 1-5-(hydromethyl)teterahydrofuran-2-yl-5-methylpyrimidine-2,4(1*H*,3*H*)-dione, along with thymine as the degradation products of ZDV under acid conditions. Multiple other publications exist in the literature on stability of ZDV,[10–13] but there is no report outlining comprehensive degradation chemistry of the drug.

In the present systematic study, we detected nine degradation products of ZDV under hydrolytic and photolytic forced degradation conditions. While four were observed in stressed neutral, acidic and basic solutions, exposure of the drug to a combination of UV and visible light resulted in total seven products, with two being common. Additionally, a stress study in the solid state resulted in six degradation products, which were same to those formed during solution state stress studies. All the nine were subjected to hyphenated liquid chromatography-mass spectrometry (LC-MS) to assign the structures. At least five of them were isolated and subjected to 1D and 2D nuclear magnetic resonance (NMR) and/or infrared (IR) spectroscopy for further confirmation of their structures. The results and observations allowed outlining of degradation pathway of the drug under the investigated stress conditions.

A significant finding was the formation of 3′-amino-3′-deoxythymidine (AMT) upon base hydrolysis and photolysis of ZDV. This degradation product is a known catabolite of the drug and is reported to exhibit high degree of toxicity towards human hemopoietic cells.[14–16] The toxicity of all other characterised degradation products was also predicted using TOPKAT software.

In recent years, intensive global efforts have led to increased number (~17 million) of people receiving life-long HIV treatment.[17] Owing to this reason, the presence of HIV drugs and their related substances in environmental matrices has come under recent focus.[18] Hence the results of this study assumingly are important even with respect to the fate of ZDV in the environment.

Department of Pharmaceutical Analysis, National Institute of Pharmaceutical Education and Research (NIPER), Sector 67, S.A.S. Nagar 160 062, Punjab, India. E-mail: ssingh@niper.ac.in; Fax: +91 172 2214692; Tel: +91 172 2214682

† Electronic supplementary information (ESI) available. See DOI: 10.1039/c7ra00678k

Experimental

Chemicals and reagents

Pure ZDV was obtained as a gratis sample from M/S Aurobindo Pharma Ltd. (Hyderabad, India). Hydrochloric acid (HCl) and sodium hydroxide (NaOH) were purchased from LOBA Chemie Pvt. Ltd. (Mumbai, India) and Ranbaxy Laboratories (S.A.S. Nagar, India), respectively. HPLC grade methanol (CH_3OH) was purchased from Aldrich (St. Louis, MO, USA). Deuterated methanol (CD_3OD) of 99.8% atom D purity was also purchased from Aldrich. Buffer salts and all other chemicals were of analytical reagent grade. Ultra pure water (H_2O) was obtained from ELGA water purification unit (Bucks, England).

Apparatus and equipments

Accelerated stability studies were carried out in humidity (KBF720, WTC Binder, Tuttlingen, Germany) and photostability (KBWF240, WTC Binder, Tuttlingen, Germany) chambers set at 40 °C/75% RH and 25 °C, respectively. The photostability chamber was equipped with an illumination bank on inside top consisting of a combination of three UV (OSRAM L18 W/73) and three white fluorescent (Philips, Trulite) lamps. Lux meter (model ELM 201, Escorp, New Delhi, India) and near UV radiometer (model 206, PRC Krochmann GmbH, Berlin, Germany) were used to measure visible illumination and near UV energy, respectively.

HPLC studies were carried out on LC-2010C HT liquid chromatograph (Shimadzu, Kyoto, Japan), which was equipped with a SPD-M20A prominence diode array detector. Pursuit XRs LC column (5 μ, C18, 250 × 4.6 mm, Varian Inc., Lake Forest, CA, USA) was used for analytical studies, while Kingsorb column (5 μ, C18, 250 × 10.0 mm, Phenomenex, Torrance, CA, USA) was used for isolation of the degradation products.

Liquid chromatography-high resolution mass spectrometry (LC-HRMS) studies were carried out using LC-ESI-Q-TOF-MS, in which LC part consisted of 1100 series HPLC (Agilent Technologies, Waldbronn, Germany) comprising of an on-line degasser (G1379A), binary pump (G1312A), auto injector (G1313A), column oven (G1316A) and a PDA detector (G1315B). The HRMS system consisted of MicrOTOF-Q spectrometer (Bruker Daltonics, Bremen, Germany). System control and data acquisition were done by Hystar software (version 3.1) from the same source. The calibration solution used was 5 mM sodium formate. Liquid chromatography-multistage mass spectrometry (LC-MS^n) data were acquired on Accela LC that was connected to a linear trap quadrupole mass spectrometer LTQ-XL-MS 2.5.0 (Thermo, San Jose, CA, USA). The mass spectra were acquired and processed using Xcalibur software (version 2.0.7 SP1). NMR studies were performed on JNM-ECA 500 MHz NMR spectrometer (JEOL, Tokyo, Japan). The data were processed by Delta v5.0.4.4 software. IR spectra of the drug and the selected degradation products were recorded on Spectrum Two IR spectrometer (Perkin Elmer, Waltham, MA, USA).

pH/Ion analyzer model PB-11 from Sartorius (Goettingen, Germany) was used to check pH of all the solutions. Other equipments used were sonicator (3210, Branson Ultrasonics Corporation, Danbury, CT, USA), precision analytical balance (AG 135, Mettler Toledo, Schwerzenbach, Switzerland) and auto pipettes (Eppendorf, Hamburg, Germany).

Solution stress degradation studies

The drug was subjected to hydrolytic, oxidative and photolytic solution stress studies according to the protocol described in our previous publications.[19,20] Final drug concentration in all the stress solutions was 2 mg ml^{-1}. Hydrolytic studies were carried out in water (neutral), 1 N HCl and 1 N NaOH solutions. The temperature of hydrolytic reactions was 80 °C. Oxidative stress studies were conducted in 15% H_2O_2 solution and in the presence of 100 mM% AIBN (200 mM% AIBN solution in CH_3-CN : CH_3OH (80 : 20) diluted with equal volume of drug stock solution in water (4 mg ml^{-1})). Photolytic study was conducted on the drug solution prepared in water. The same was exposed to 1.2 million lx h cool white and 200 W h m^{-2} UV-A radiations. Samples were neutralized with acid/alkali and/or diluted two times with water before injecting into HPLC. The HPLC method involved a mobile phase composed of methanol (A) and 10 mM ammonium formate (pH 3.75) (B) that was run in a gradient mode (T_{min}/%B; T_0/95; T_5/95; T_{50}/10; T_{55}/95; T_{62}/95). The column oven temperature was 30 °C. The detection wavelength,

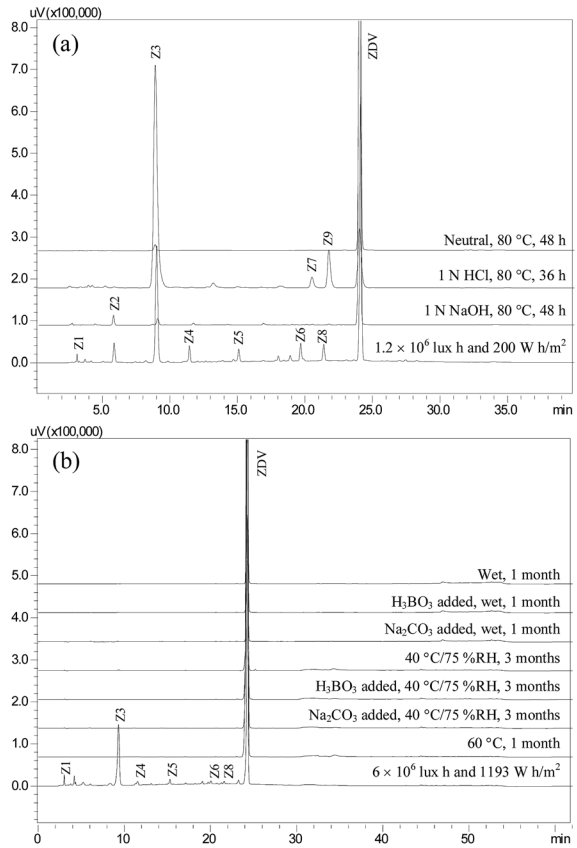

Fig. 1 Chromatograms showing degradation products of zidovudine (ZDV) formed in solution (a) and solid state (b) stress conditions.

flow rate and injection volume were 254 nm, 1 ml min^{-1} and 10 μl, respectively.

Solid state stress studies

Four sets were prepared for solid state stress investigations. The first and second sets were further divided into three subsets, *i.e.*, ZDV; ZDV : H_3BO_3 (1 : 2), and ZDV : Na_2CO_3 (1 : 2). The first set (all three subsets) contained the drug and stressors along with 50 μl H_2O in closed vials, and was charged to accelerated stability test chamber for 1 month. The second set (three subsets) was exposed to accelerated stability condition of 40 °C/75% RH for 3 months in an open container. The third set containing drug alone in cotton-plugged ampoules was kept at 60 °C for 1 month. The fourth set comprised of the drug in open Petri dish, which was charged to photostability chamber for a sufficient duration so as to provide a total dose of 6 million lx h cool white light and 1193 W h m^{-2} near-UV. After completion of the study, all the samples were withdrawn and diluted in water to a final concentration of 2 mg ml^{-1}. The samples were monitored for chemical changes by HPLC using the same method that was employed for evaluation of the solution state stressed samples, except that the injection volume was halved to 5 μl.

LC-HRMS and LC-MS^n studies

The LC method used for MS studies was similar to the HPLC method employed for analyses of the stressed samples. However, to prevent condensation in the ionization source, the solvent flow into MS system was reduced from 1 ml min^{-1} to 200 μl min^{-1}, using a diversion valve. The HRMS and MS^n instrument parameters were optimized suitably to obtain best intensity of the molecular ions (Table S1†). LC-MS^n studies were conducted by defining the segments for individual degradation products.

NMR studies on the drug and selected degradation products

The drug itself was initially subjected to 1D and 2D NMR studies in CD_3OD to compare its spectra with those of the degradation

Table 1 HRMS and MS^n data of zidovudine (ZDV) and its degradation products **Z1–Z9**

	HRMS data				MS^n data	
	Accurate mass	Exact mass	Error (mmu)	Accurate masses of fragments	Precursor ion	Product ion(s)
$[ZDV + H]^+$	268.1042	268.1040	0.2	225.0848, 207.0747, 127.0515	268	225, 127[a]
					268 → 225	207[a], 127[a]
$[\mathbf{Z1} + H]^+$	240.0969	240.0979	−1.0	223.0712, 193.0623, 127.0635	240	223, 193[a], 127[a]
					240 → 223	193[a], 127[a]
$[\mathbf{Z2} + H]^+$	242.1134	242.1135	−0.1	225.0867, 207.0761, 127.0482	242	225, 127[a]
					242 → 225	207[a], 127[a]
$[\mathbf{Z3} + H]^+$	127.0522	127.0502	2.0	—	127[a]	
$[\mathbf{Z4} + H]^+$	366.1360	366.1408	−4.8	251.0842, 242.1095, 240.0918, 214.0815, 196.0705, 184.0681, 142.0614	MS^n data were similar to the fragment of *m*/*z* 366 of degradation product **Z6** as shown below	
$[\mathbf{Z5} + H]^+$	270.1071	270.1084	−1.3	144.0659, 127.0567	270	144[a], 127[a]
$[\mathbf{Z6} + H]^+$	507.1968	507.1946	2.2	392.1345, 381.1502, 366.1406, 355.1364, 337.1254, 325.1256, 283.1130, 266.0879, 251.0764, 242.1122, 223.0657, 214.0944, 205.0687	507	392, 381, 366, 355, 283, 266, 251, 242, 240, 223, 205[a]
					507 → 392	251
					507 → 381	283, 266, 240, 223, 205[a], 142, 125[a]
					507 → 366	251, 242, 240, 214, 142, 125[a], 116[a]
					507 → 355	337[a], 325, 266, 223, 214, 196[a], 184[a], 125[a]
					507 → 325	184[a]
					507 → 283	266, 223, 142, 125[a]
					507 → 266	223, 125[a]
					507 → 251	127[a]
					507 → 242	116[a]
					507 → 240	142, 125[a]
					507 → 223	205[a], 153[a], 125[a]
					507 → 214	196[a], 184[a]
					507 → 142	125[a]
$[\mathbf{Z7} + H]^+$	268.1017	268.1040	−2.3	225.0870, 127.0520	MS^n data were similar to the drug (ZDV), as shown above	
$[\mathbf{Z8} + H]^+$	272.0841	272.0877	−3.6	127.0482	272	212[a], 127[a]
$[\mathbf{Z9} + H]^+$	268.1029	268.1040	−1.1	225.0848, 207.0744, 127.0515	MS^n data were similar to the drug (ZDV), as shown above	

[a] Fragments were not captured for further MS^n studies.

products, in order to characterize the latter. Five out of the nine degradation products were enriched and isolated using semi-preparative HPLC by employing suitable HPLC methods. The mobile phase used for isolation contained methanol and acidified water. In each case, the collected HPLC fraction was dried on a rotary evaporator and the residue was subjected to 1D and 2D NMR studies after preparing solution in CD_3OD. Pre-saturation method was used to suppress the signal due to water.

IR studies on the drug and isolated degradation products

The IR spectra of the drug and certain isolated degradation products were recorded in KBr.

In silico toxicity prediction

TOPKAT (TOxicity Prediction by Komputer Assisted Technology, Discovery Studio 2.5, Accelrys, Inc., San Diego, CA, USA) was employed to predict potential toxicity of the degradation products.[21] The software employs statistically robust and cross-validated quantitative structure toxicity relationship (QSTR) models to predict toxicological end points in term of probability values. To develop the models, it uses a range of two-dimensional molecular, electronic and spatial descriptors. The program applies the patented optimal predictive space (OPS) validation method to estimate the assurance in the prediction. Probability values from 0.0 to 0.30 are considered as low probabilities for any toxicological end point, whereas those greater than 0.70 are considered as high probabilities.[22] The values from 0.3 to 0.7 fall in an in-determinate zone.

Results and discussion

Solution state degradation behaviour of the drug

In total nine degradation products (**Z1–Z9**) were detected under various solution stress conditions (Fig. 1a). In neutral hydrolytic condition (80 °C, 48 h), only one degradation product **Z3** was formed, while stressing under acidic condition (1 N HCl, 80 °C, 36 h) resulted in **Z3**, **Z7** and **Z9**. In basic stress condition (1 N NaOH, 80 °C, 48 h), the drug primarily degraded to **Z2** and **Z3**. Exposure of the drug to UV and visible light resulted in seven products, *viz.*, **Z1–Z6** and **Z8**. The drug proved to be stable upon oxidative stress.

Solid state degradation behaviour of the drug

No degradation of the drug was observed in the first three sets of the four subjected to solid state stress studies. The drug showed instability in the fourth set, which was subjected to light, and resulted in **Z3** as a major degradation product. Additionally, **Z1**, **Z4–Z6**, and **Z8** were formed, but only in detectable amounts (Fig. 1b).

Mass spectrometric studies on the drug

HRMS line spectrum of ZDV (Fig. S1a†) showed accurate mass of *m*/*z* 268.1042, which had difference of 0.2 mmu with respect to the exact mass of 268.1040 Da (Table 1). As divulged by MS^n studies, the drug molecular ion fragmented into product ion of

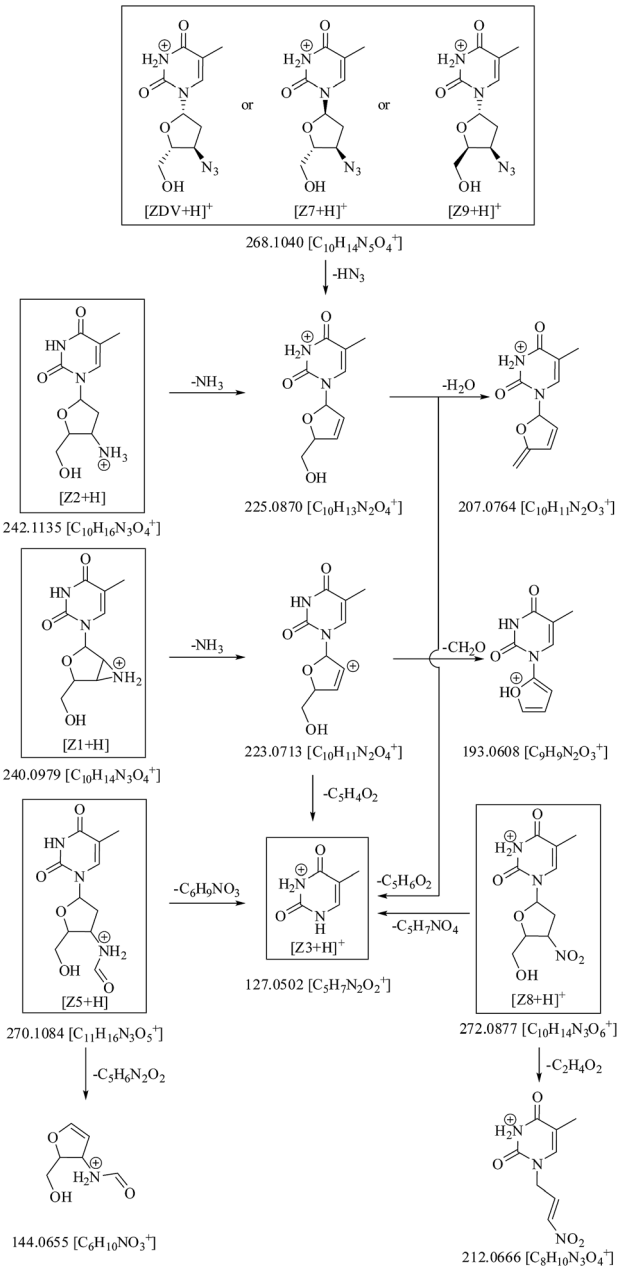

Fig. 2 Mass fragmentation pathway of zidovudine (ZDV) and its degradation products **Z1–Z3**, **Z5** and **Z7–Z9** (solid boxes) under ESI +ve mode.

m/*z* 225 on loss of HN_3. The latter ion further dissociated into fragments of *m*/*z* 207 and 127 on loss of H_2O and $C_5H_6O_2$, respectively (Fig. 2).

NMR spectroscopic studies on the drug

NMR spectroscopy studies on the drug were carried out in CD_3OD. The resultant 1D and 2D NMR spectra are shown in Fig. S2,† while corresponding data are compiled in Table 2. ^1H NMR spectrum showed a total of eleven non-labile protons, whereas the remaining two labile hydrogens were not observed due to H/D exchange. The following were the observed signals: (i) a singlet of methine proton of pyrimidine ring of position H-6

Table 2 ^{1}H, COSY, ^{13}C, DEPT-135, HSQC and HMBC data of zidovudine (ZDV) in CD_3OD[a]

Structure	Position	^{1}H (δ ppm)	COSY	^{13}C (δ ppm)	DEPT-135	HSQC	HMBC
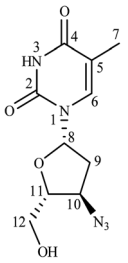	2	—	—	150.96	—	—	—
	4	—	—	165.06	—	—	—
	5	—	—	110.27	—	—	—
	6	7.78 (s)	H-7	136.74	CH	C-6	C-2, 4, 7, 8
	7	1.86 (s)	H-6	11.12	CH_3	C-7	C-4, 5, 6
	8	6.15 (t)	H-9	84.70	CH	C-8	C-2, 6
	9	2.34–2.42 (m)	H-8, 10	36.93	CH_2	C-9	C-8, 10, 11
	10	4.32–4.36 (m)	H-9, 11	60.32	CH	C-10	C-8, 11
	11	3.88–3.90 (m)	H-10, 12a, b	84.74	CH	C-11	*
	12a, b	3.71–3.74 (m), 3.80–3.83 (m)	H-11	61.07	CH_2	C-12	C-10

[a] Signals were not observed; d, doublet; s, singlet, and m, multiplet.

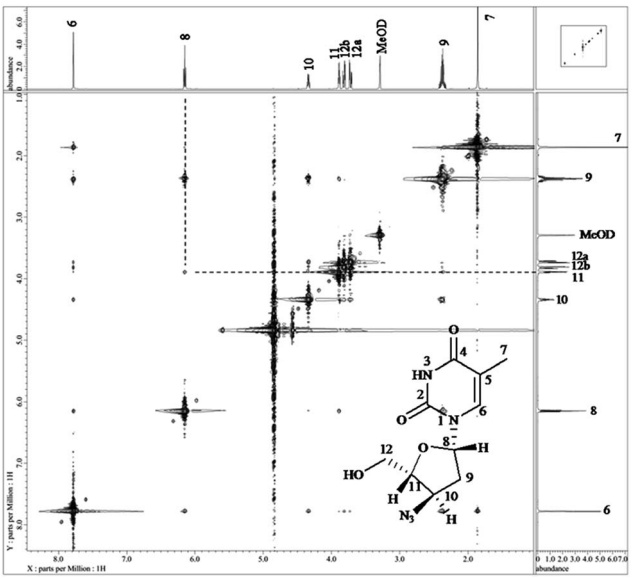

Fig. 3 NOESY spectrum of zidovudine (ZDV) showing correlation between protons H-8 and H-11.

at δ 7.78 ppm; (ii) one singlet at δ 1.86 ppm corresponding to methyl protons of position H-7; (iii) a triplet at δ 6.15 ppm for methine proton of position H-8; (iv) multiplet at δ 2.34–2.42 ppm for methylene protons of position H-9; (v) two multiplets at δ 4.32–4.36 ppm and δ 3.88–3.90 ppm for methine proton of positions H-10 and H-11, respectively, and (vi) two pairs of multiplets at δ 3.71–3.74 ppm and δ 3.80–3.83 ppm for non-equivalent methylene protons of position H-12.

^{13}C NMR spectrum showed a total of ten carbons in the structure. The positions of methylene, methyl and methine carbons were differentiated using DEPT-135. Two signals arose at δ 150.96 ppm and δ 165.06 ppm for carbonyl carbons of positions C-2 and C-4, respectively. A single signal was observed at δ 110.27 ppm for quaternary carbon C-5. One methyl carbon corresponding to position C-7 was observed at δ 11.12 ppm. The signals for tertiary carbons, *viz.*, C-6, C-8, C10 and C-11 arose at δ 136.74 ppm, δ 84.70 ppm, δ 60.32 ppm and δ 84.74 ppm, respectively. Another set of signals for two methylene carbons were observed at δ 36.93 ppm (C-9) and δ 61.07 ppm (C-12). While 2D (COSY, HSQC and HMBC) data helped to assign the connectivities between the atoms, stereochemistry of positions 8, 10 and 11 was confirmed by NOESY spectrum (Fig. 3). H-8 showed NOE correlations with H-11, which confirmed that both the protons were in the same plane, while absence of correlation between H-8 and H-10 indicated their presence in an opposite plane.

IR studies on the drug

IR spectrum of the drug (Fig. S3a†) showed bands for N–H stretching at 3463 cm^{-1}, C–H stretching at 2932 cm^{-1}, azide stretching at 2083 cm^{-1} (characteristic), two C=O stretching bands near 1687 cm^{-1}, while scissoring, twisting, wagging and rocking vibrations were observed below 1500 cm^{-1}.

Characterization of the degradation products Z1–Z9

The degradation products **Z1–Z9** were characterized based on HRMS, MS^n, NMR and IR results. HRMS line spectra of all the degradation products are shown in Fig. S1b–j,† while their accurate and exact masses and errors (mmu) along with MS^n data are included in Table 1. NMR data were obtained for the degradation products **Z5–Z9** (Table 3), while IR spectra were recorded for **Z5**, **Z7** and **Z9** (Fig. S3b–d,† respectively). The characterization of the degradation products is discussed below individually or in groups, categorized on the basis of similarities in their structures.

Z1. The mass to charge ratio of **Z1** was observed to be 240.0969 Da. Its molecular formula worked out as $C_{10}H_{14}N_3O_4^+$, with exact mass of 240.0979 Da (error −1.0 mmu). The proposed structure and fragmentation pattern are shown in Fig. 2. The molecular ion fragmented in MS^2 step into product ion of *m*/*z* 223 on loss of NH_3, which on MS^3 run reduced into fragments of *m*/*z* 193 and 127 on loss of CH_2O and $C_5H_4O_2$, respectively. The product was characterized as 1-(4-(hydroxymethyl)-3-oxa-6-azabicyclo[3.1.0]hexan-2-yl)-5-methylpyrimidine-2,4(1*H*,3*H*)-dione. It was previously proposed by us as an intermediate in the process of degradation of ZDV into thymine,[7] but was not characterized

Table 3 ^{1}H, COSY, ^{13}C, DEPT-135, HSQC and HMBC data of ZDV degradation products **Z5–Z9** in CD_3OD[a]

Structure	Position	^{1}H (δ ppm)	COSY	^{13}C (δ ppm)	DEPT-135	HSQC	HMBC
Z5	2	—	—	151.00	—	—	—
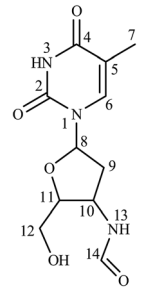	4	—	—	165.11	—	—	—
	5	—	—	110.23	—	—	—
	6	7.86 (s)	H-7	136.77	CH	C-6	C-2, 4, 7, 8
	7	1.87 (s)	H-6	11.11	CH_3	C-7	C-4, 5, 6
	8	6.22 (t)	H-9	84.55	CH	C-8	C-2, 6
	9	2.27–2.39 (m)	H-8, 10	37.43	CH_2	C-9	C-8, 10, 11
	10	4.55–4.56 (m)	H-9, 11	47.67	CH	C-10	C-12
	11	3.85–3.87 (m)	H-10, 12a, b	85.14	CH	C-11	C-10
	12a, b	3.71–3.74 (m), 3.82–3.85 (m)	H-11	60.96	CH_2	C-12	C-10
	14	8.06 (s)		162.42	CH	C-14	C-10
Z6	2	—	—	150.42	—	—	
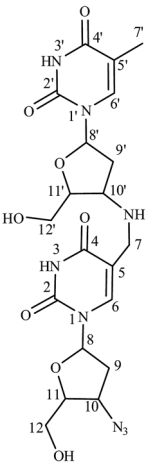	2′	—	—	150.95	—	—	
	4	—	—	163.74	—	—	
	4′	—	—	165.01	—	—	
	5	—	—	104.43	—	—	
	5′	—	—	110.53	—	—	
	6	8.31 (s)	—	142.93	CH	C-6	C-2, 4, 7, 8
	6′	7.75 (s)	H-7′	136.83	CH	C-6′	C-2′, 4′, 7′, 8′
	7	3.97 (s)	—	42.84	CH_2	C-7	C-4, 5, 6, 10′
	7′	1.87 (s)	H-6′	11.11	CH_3	C-7′	C-4′, 5′, 6′
	8	6.14 (t)	H-9	85.45	CH	C-8	C-6
	8′	6.30 (t)	H-9′a, b	85.02	CH	C-8′	C-2′, 6′
	9	2.43–2.49 (m)	H-8, 10	37.35	CH_2	C-9	C-10
	9′a, b	2.54–2.60 (m), 2.69–2.73 (m)	H-8′, 10′	34.58	CH_2	C-9′	C-8′, 11′
	10	4.37 (q)	H-9, 11	59.94	CH	C-10	C-8, 11
	10′	4.00–4.04 (m)	H-9′, 11′	57.37	CH	C-10′	*
	11	3.92–3.93 (m)	H-10, 12	85.16	CH	C-11	*
	11′	4.25–4.29 (m)	H-10′, 12a′, b′	82.15	CH	C-11′	*
	12	3.85–3.87 (m)	H-11	60.84	CH_2	C-12	*
	12a′, b′	3.74–3.77 (m), 3.88–3.90 (m)	H-11′	61.28	CH_2	C-12′	C-11′
Z7	2	—	—	150.60	—	—	—
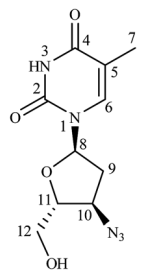	4	—	—	164.91	—	—	—
	5	—	—	110.61	—	—	—
	6	7.69 (s)	H-7	136.55	CH	C-6	C-2, 4, 7, 8
	7	1.88 (s)	H-6	11.02	CH_3	C-7	C-4, 5, 6
	8	5.66–5.69 (m)	H-9a, b	79.99	CH	C-8	C-2, 6
	9a, b	1.94–1.97 (m), 2.11–2.18 (m)	H-8, 10	29.25	CH_2	C-9	C-8, 10, 11
	10	3.61–3.65 (m)	H-9a, b, 11	58.29	CH	C-10	*
	11	3.86 (s)	H-10, 12a, b	65.69	CH	C-11	C-9, 10
	12a, b	3.72–3.75 (m), 4.01–4.04 (m)	H-11	70.34	CH_2	C-12	C-8, 10, 11
Z8	2	—	—	150.95	—	—	—
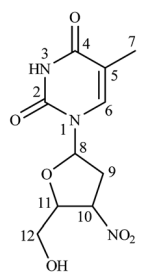	4	—	—	164.97	—	—	—
	5	—	—	110.65	—	—	—
	6	7.78 (s)	H-7	136.57	CH	C-6	C-2, 4, 7, 8
	7	1.87 (s)	H-6	11.10	CH_3	C-7	C-4, 5, 6
	8	6.37 (t)	H-9a, b	85.25	CH	C-8	C-2, 6
	9a, b	2.48–2.54 (m), 2.95–3.00 (m)	H-8, 10	35.74	CH_2	C-9	C-8, 10
	10	5.30–5.33 (m)	H-9a, b, 11	83.83	CH	C-10	C-8
	11	4.48–4.49 (m)	H-10, 12	85.39	CH	C-11	*
	12	3.81–3.89 (m)	H-11	61.87	CH_2	C-12	C-10

Table 3 (*Contd.*)

Structure	Position	^{1}H (δ ppm)	COSY	^{13}C (δ ppm)	DEPT-135	HSQC	HMBC
Z9 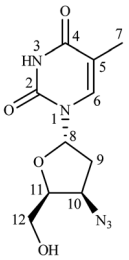	2	—	—	150.70	—	—	—
	4	—	—	164.88	—	—	—
	5	—	—	110.55	—	—	—
	6	7.48 (s)	H-7	136.38	CH	C-6	C-2, 4, 7, 8
	7	1.85 (s)	H-6	11.00	CH_3	C-7	C-4, 5, 6
	8	5.76–5.79 (m)	H-9a, b	77.39	CH	C-8	C-2, 6
	9a, b	1.93–1.97 (m), 2.07–2.12 (m)	H-8, 10	33.34	CH_2	C-9	C-8, 10, 11
	10	4.14–4.15 (m)	H-9, 11	60.91	CH	C-10	C-8, 11
	11	3.97–4.01 (m)	H-10, 12	66.71	CH	C-11	C-10, 12
	12a, b	3.72–3.77 (m), 3.81–3.84 (m)	H-11	66.41	CH_2	C-12	C-8, 10, 11

[a] Signals were not observed. Key: d, doublet; m, multiplet; s, singlet, and q, quartet.

experimentally at that time. Thus our previous hypothesis stands confirmed through characterization of the same intermediate in this study.

Z2. It was formed on base hydrolysis as well as on exposure of the drug solution to ICH recommended dose of light in a photostability chamber. Its accurate and exact masses were 242.1134 and 242.1135 Da, respectively (error = −0.1 mmu). The molecular formula for the product was determined to be $C_{10}H_{16}N_3O_4^+$. It was characterized as 3′-amino-3′-deoxythymidine (AMT) (Fig. 2). This product is previously reported as a metabolite of the drug.[23,24] The parent of *m*/*z* 242 fragmented into product ion of *m*/*z* 225 on loss of NH_3, which further showed losses of H_2O and $C_5H_6O_2$ to result into fragment species of *m*/*z* 207 and 127, respectively.

Z3. This was formed as a major degradation product under almost all the stress conditions. Its accurate mass was determined to be 127.0522 Da, whereas exact mass calculated out to be 127.0502 Da (error = 2 mmu). The molecular formula was found to be $C_5H_7N_2O_2^+$. These data helped in characterization of the product as 5-methyluracil (thymine, Fig. 2). The same is mentioned as an impurity in multiple compendial monographs.[25–27] Even we detected **Z3** as the major degradation product of the drug in our earlier studies.[7,8]

Z4 and Z6. $[\mathbf{Z4} + H]^+$ and $[\mathbf{Z6} + H]^+$ had accurate masses of 366.1360 and 507.1968 Da; exact masses of 366.1408 (error = −4.8 mmu) and 507.1946 Da (error = 2.2 mmu); and molecular formulae $C_{15}H_{20}N_5O_6^+$ and $C_{20}H_{27}N_8O_8^+$, respectively. The characterized structures of both the products, along with their fragmentation behaviour, are shown in Fig. 4. The product **Z6** was postulated as 1-(4-azido-5-(hydroxymethyl)tetrahydrofuran-2-yl)-5-((2-(hydroxymethyl)-5-(5-methyl-2,4-dioxo-3,4-dihydropyrimidin-1(2*H*)-yl)tetrahydrofuran-3-ylamino)methyl)pyrimidine-2,4(1*H*,3*H*)-dione. Its generation involved interaction of the methyl group of one drug molecule with the azide moiety of another, releasing N_2 in the process.

Fig. 4 shows that molecular ion of **Z6** fragmented into product ions of *m*/*z* 392, 381, 366 and 355 on the loss of $C_5H_9NO_2$, $C_5H_6N_2O_2$, $C_5H_7N_3O_2$ and $C_7H_8N_2O_2$, respectively. Of these, the species of *m*/*z* 366 had the same mass as molecular ion of **Z4**. The precursor ion of *m*/*z* 392 fragmented into product ion of *m*/*z* 251 on loss of $C_5H_7N_3O_2$. The latter product ion was also formed from fragment of *m*/*z* 366 on loss of $C_5H_9NO_2$. The ion of *m*/*z* 381 reduced into species of *m*/*z* 283 and 240 on loss of $C_5H_6O_2$ and $C_5H_7N_3O_2$, respectively. The precursor of *m*/*z* 283 further degraded *via* routes: (i) *m*/*z* 283 → 266 (loss of NH_3) → 223 (loss of HN_3) → 205, 153 and 125 (on loss of H_2O, C_4H_6O and $C_5H_6O_2$, respectively) and (ii) *m*/*z* 283 → 142 (loss of $C_5H_7N_3O_2$) → 125 (loss of NH_3). The fragment of *m*/*z* 366 also dissociated into product ions of *m*/*z* 251 and 240 on loss of $C_5H_9NO_2$ and $C_5H_6N_2O_2$, respectively, along with ions of *m*/*z* 242 and 214 on loss of $C_5H_4N_2O_2$ and $C_7H_8N_2O_2$, respectively. The precursor of *m*/*z* 242 further reduced into fragment of *m*/*z* 116 on loss of $C_5H_6N_2O_2$, while the precursor of *m*/*z* 214 dissociated into ions of *m*/*z* 196 and 184 on loss of H_2O and CH_2O, respectively. Another MS^2 product ion of *m*/*z* 355 fragmented into species of *m*/*z* 337, 325 and 266 on loss of H_2O, CH_2O and $C_3H_7NO_2$, respectively. The fragment of *m*/*z* 325 reduced into ion of *m*/*z* 184 on loss of $C_5H_7N_3O_2$.

The mass fragmentation spectra of **Z6** and **Z4** were overlapping beyond *m*/*z* 366 (Table 1, Fig. S1†). Therefore, **Z4** was indicated to be breakdown product of **Z6** arising on loss of 4-azido-5-(hydroxymethyl)tetrahydrofuran-2-yl moiety. Its structure was proposed as 1-(4-((2,4-dioxo-1,2,3,4-tetrahydro pyrimidin-5-yl) methylamino)-5-(hydroxymethyl)tetrahydro furan-2-yl)-5-methylpyrimidine-2,4(1*H*,3*H*)-dione.

Due to unusual structure of **Z6**, and it being precursor to generation of **Z4**, therefore, it was considered prudent to confirm its structure by ^{1}H, COSY, ^{13}C, DEPT-135, HSQC and HMBC NMR studies. The spectra are shown in Fig. S4† and corresponding data are compiled in Table 3. The following were the key observations: (i) twenty one protons appeared in ^{1}H NMR spectrum of **Z6** (Fig. S4a†) against eleven in the drug (Fig. S2a†), highlighting that **Z6** was truly formed *via* interaction of two ZDV molecules; (ii) two signals were observed corresponding to individual signal of proton(s) in the drug molecule, except methyl protons, where only one signal was observed (Fig. S4a *versus* S2a†); (iii) DEPT-135 experiment substantiated that specific signal at δ 3.97 ppm appeared because of

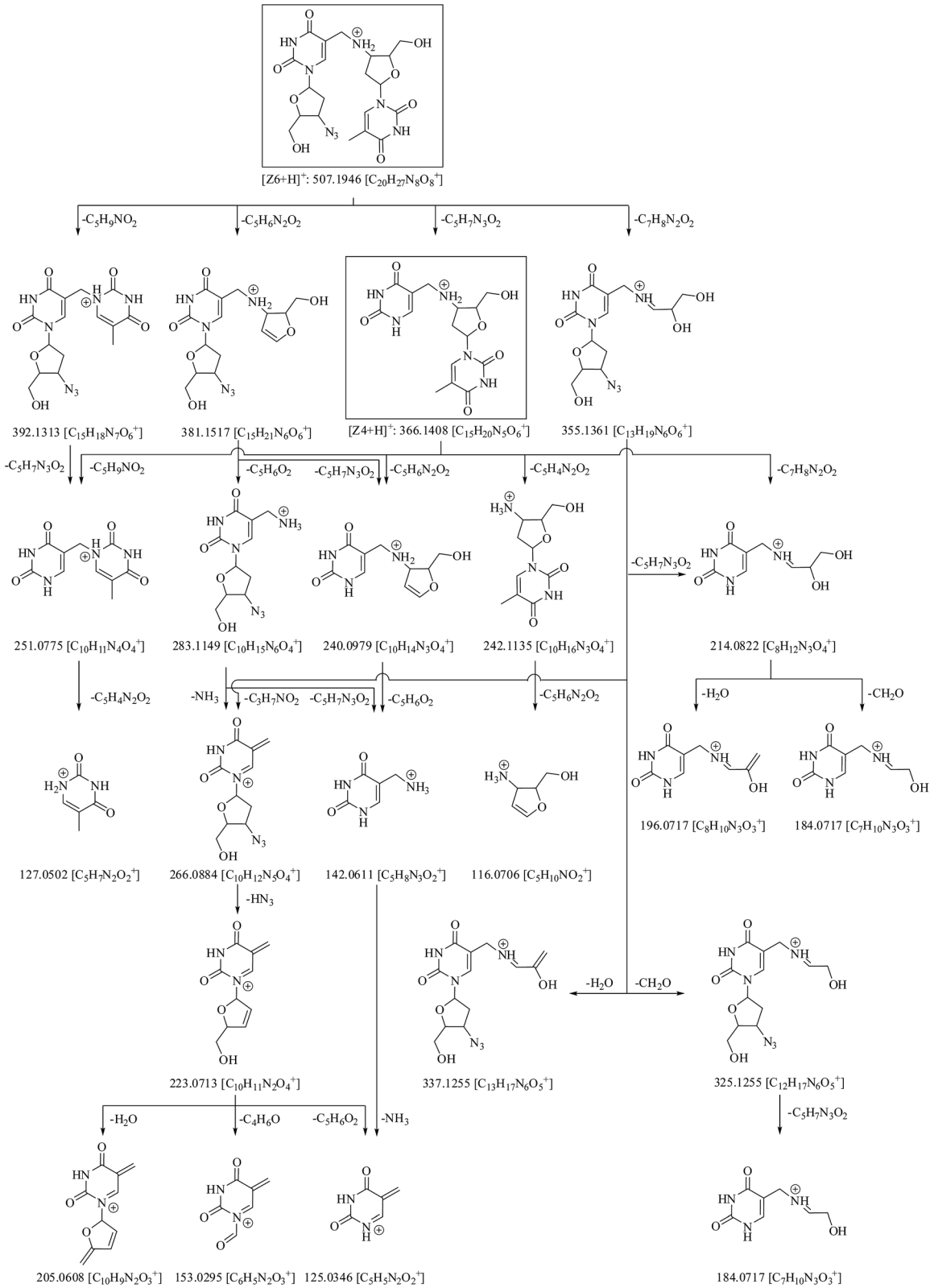

Fig. 4 Structures and fragmentation behaviour of degradation products **Z4** and **Z6** (solid boxes). Fragments of *m*/*z* 153, 127, 125 and 116 were observed only during MS^n study.

methylene protons in **Z6** (Fig. S4a and c†), and (iv) HMBC data showed connectivity of H-7 to C-10′, thus supporting coupling of two molecules *via* methylene and amino groups.

Z5. The molecular ion of **Z5** had accurate and exact masses as 270.1071 and 270.1084 Da, respectively (error −1.3 mmu). The molecular formula worked out to be $C_{11}H_{16}N_3O_5^+$. On collision

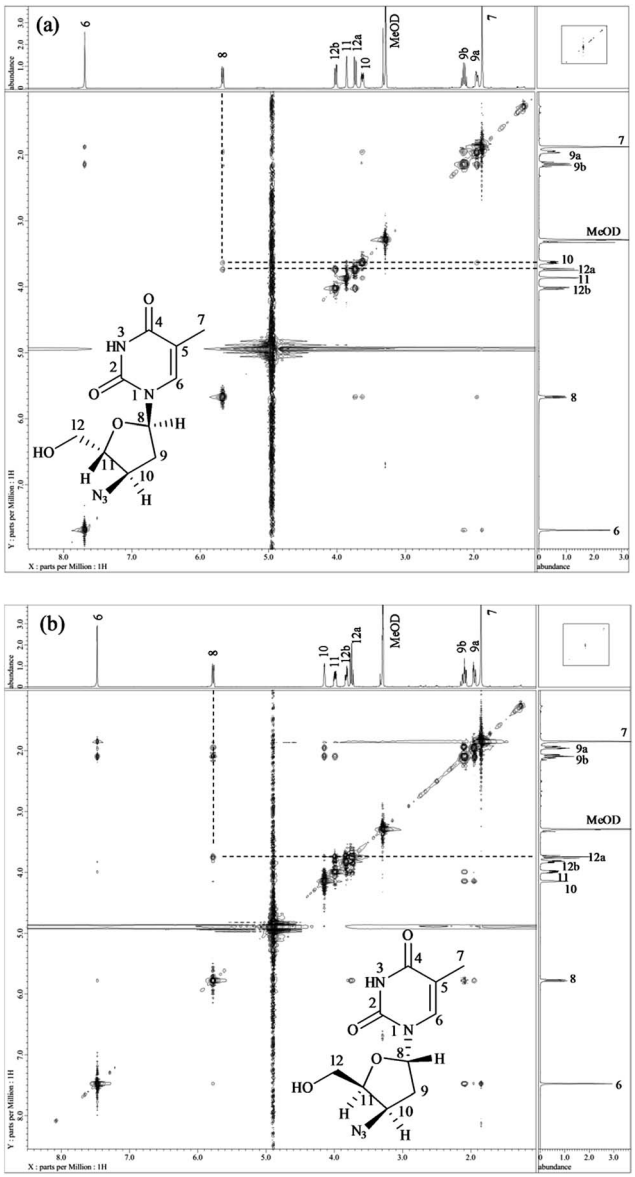

Fig. 5 NOESY spectra of degradation products **Z7** (a) and **Z9** (b) showing correlation of proton H-8 with H-10, 12a in **Z7** and H-8 with 12a in **Z9**.

induced dissociation, it formed product ions of *m*/*z* 144 and 127 on loss of $C_5H_6N_2O_2$ and $C_6H_9NO_3$, respectively. The structure was assigned as *N*-(2-(hydroxymethyl)-5-(5-methyl-2,4-dioxo-3,4-dihydropyrimidin-1(2*H*)-yl)tetrahydrofuran-3-yl)formamide (Fig. 2). The same was confirmed through 1D and 2D NMR results (Fig. S5†, Table 3). Twelve protons appeared in the ^{1}H NMR spectrum (Fig. S5a†) in comparison to eleven in case of the drug (Fig. S2a†). The change in the azide group was highlighted through chemical shift values of ^{1}H (δ 4.55–4.56 ppm) and ^{13}C (δ 47.67 ppm) for position 10 as compared to the drug (δ 4.32–4.36 ppm and δ 60.32 ppm, respectively) (Table 3). The addition of CHO and removal of N_2, which was highlighted by HRMS results, was confirmed by one additional signal for ^{1}H and ^{13}C at δ 8.06 and 162.42 ppm, respectively. The same was substantiated by HMBC data where H-14 showed connectivity with C-10 (Fig. S5e†). The structure was further supported by IR spectrum (Fig. S3b†), in which absorption band of azide (~2083 cm^{-1}) was absent as compared to the drug spectrum (Fig. S3a†).

Z7 and Z9. Accurate masses of $[\mathbf{Z7} + H]^+$ and $[\mathbf{Z9} + H]^+$ were 268.1017 and 268.1029 Da, respectively (Table 1). The two had same exact mass and molecular formula as the drug, *viz.*, *m*/*z* 268.1040 and $C_{10}H_{14}N_5O_4^+$, respectively. Both also showed similar fragmentation behaviour to the drug, following the route: *m*/*z* 268 → 225 (loss of HN_3) → 207, 127 (loss of H_2O, $C_5H_6O_2$, respectively) (Fig. 2). Accordingly, the two were considered to be isomeric in nature, not only among themselves, but also with respect to the drug. Characterization of their structures was attempted through ^{1}H, ^{13}C, COSY, HSQC, HMBC and NOESY NMR spectra (Table 3, and Fig. S6, S7† and 5) and also IR studies (Fig. S3c and d†).

^{1}H and ^{13}C data of both **Z7** and **Z9** were almost similar to the drug, except minor changes in chemical shifts for protons at positions H-8 to H-11. Even COSY, HSQC and HMBC correlations were similar. However, in case of **Z7**, NOE correlations of H-8 existed with positions H-10 and H-12a (Fig. 5a), which were absent in case of the drug (Fig. 3). Oppositely, similar correlation was absent between positions H-8 and H-11 that otherwise was present in the drug. This indicated that proton of H-8 was positioned in opposite plane to the drug. Hence the structure of **Z7** was characterized as 1-((2*S*,4*R*,5*R*)-4-azido-5-(hydroxymethyl) tetrahydrofuran-2-yl)-5-methyl pyrimidine-2,4(1*H*,3*H*)-dione. Against it, NOESY spectrum of **Z9** showed correlation of H-8 with H-12 (Fig. 5b), which was absent in the drug (Fig. 3). In this case, correlation of H-8 and H-11 was oppositely absent, which existed in the drug. This indicated that H-11 proton changed its plane as compared to the drug. Hence the structure of **Z9** was characterized as 1-((2*S*,4*R*,5*S*)-4-azido-5-(hydroxymethyl)tetrahydrofuran-2-yl)-5-methylpyrimidine-2,4(1*H*,3*H*)-dione. As expected, the two products had almost identical IR spectra among themselves and also to the drug (Fig. S3a *versus* c and d†).

Z8. This degradation product had accurate and exact masses of 272.0841 and 272.0877 Da (error −3.6 mmu), respectively. For the same, the molecular formula was determined as $C_{10}H_{14}N_3O_6^+$. The molecular ion in this case fragmented into product ions of *m*/*z* 212 and 127 on loss of $C_2H_4O_2$ and $C_5H_7NO_4$, respectively (Fig. 2).

1D and 2D NMR spectra of this product are shown in Fig. S8† and the data are included in Table 3. ^{1}H NMR spectrum showed signals for eleven protons, the same number as the drug. While proton of position H-10 was deshielded to δ 5.30–5.33 ppm in comparison to the drug (δ 4.32–4.36 ppm), C-10 was also shifted to higher value of δ 83.83 ppm due to the presence of nitro group at position 10, instead of the azide moiety in the drug. However, there was no difference in 2D correlations. The structure was characterized as 3′-deoxy-3′-nitrothymidine (Fig. 2). The compound is known in the literature, but not as a degradation product of ZDV.

Degradation pathway

The mechanism of formation of the major degradation product **Z3** (thymine) under hydrolytic (acid, neutral and alkaline) and

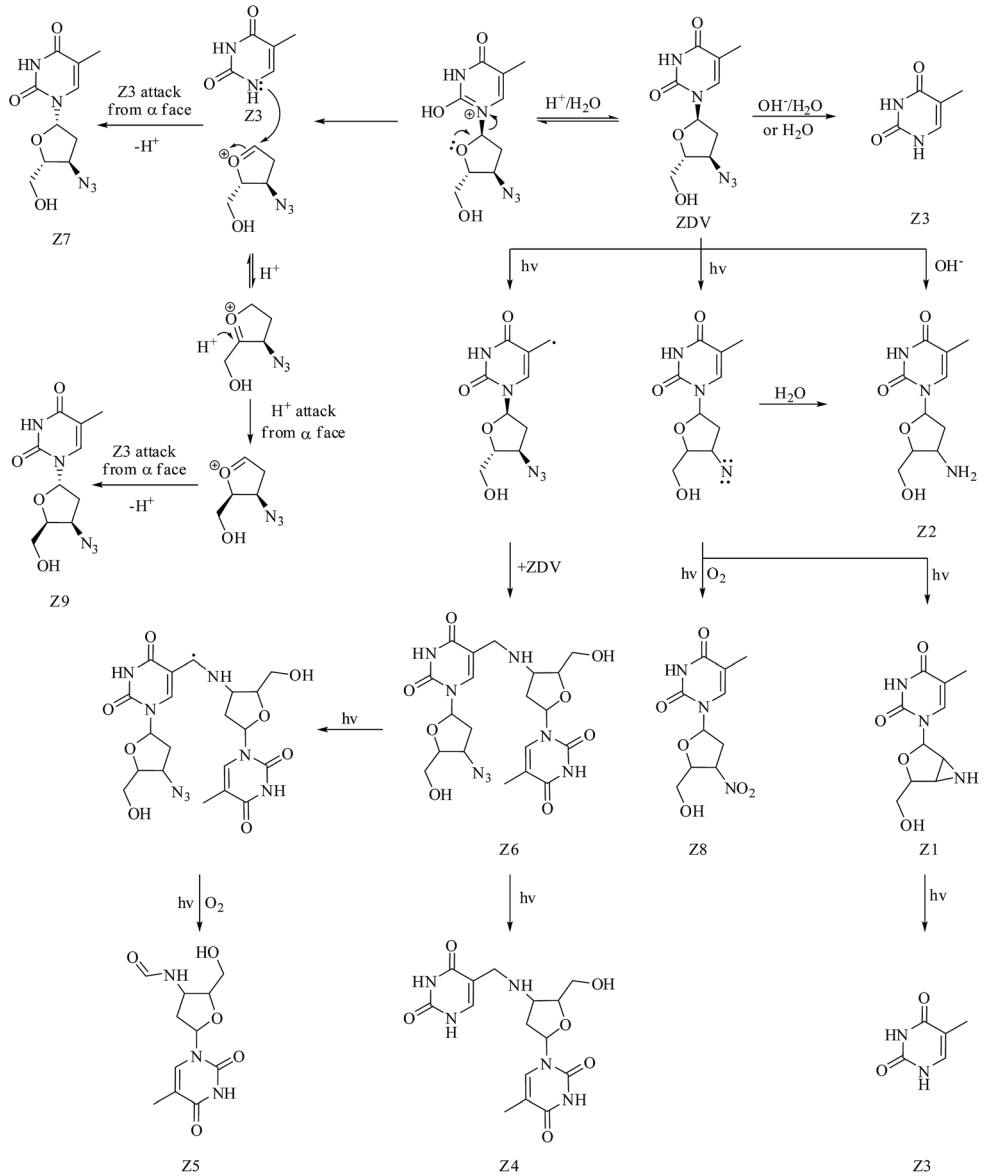

Fig. 6 Postulated degradation pathway of zidovudine (ZDV) into degradation products **Z1–Z9**.

photolytic conditions was proposed by us earlier.[7] Fig. 6 outlines the complete pathway of degradation of ZDV to products **Z1–Z9**. Formation of thymine from ZDV under acidic conditions is postulated to involve release of (2*R*,3*R*)-3-azido-2-(hydroxymethyl)-3,4-dihydro-2*H*-furanium cation. The attack of thymine back on this cation, but from α face, is the most likely explanation to the formation of **Z7**. The same cation on rearrangement to (2*S*,3*R*)-3-azido-2-(hydroxymethyl)-3,4-dihydro-2*H*-furanium cation, and again attack of thymine from the α face, explains the formation of **Z9**. The drug possesses an azide moiety and the same is well known to be responsible for the lability of the drug under photochemical conditions.[7,28,29] It is also established that azide groups undergo elimination of molecular nitrogen to generate nitrene as a reactive intermediate, which can undergo intramolecular C–H insertion reaction and photo-oxidation, leading to formation of aziridine and nitro products.[30–32] This chemistry explains formation of degradation products **Z1** and **Z8**, respectively. The conversion of nitrene intermediate (generated in the presence of light) to amine in the presence of water[33] can be considered responsible for the formation of **Z2** under photolytic conditions. Also, it is conceived that methyl group of the drug undergoes hydrogen abstraction and forms methylene radical, which interacts with azide group of another drug molecule, leading to **Z6** on the removal of N_2. **Z4** is postulated to be formed further from **Z6** on photolytic cleavage of 3-azido-2-(hydroxymethyl)-3,4-dihydro-2*H*-furyl moiety. Finally, **Z5** is probably generated upon hydrogen abstraction from methylene group of **Z6**, and photo-oxidation of the resultant methine radical.

In silico toxicity of degradation products as compared to drug

Table 4 lists *in silico* toxicity data for ZDV and its degradation products **Z1–Z9**, which were predicted using extended TOPKAT

Table 4 Data of different toxicity models of zidovudine (ZDV) and its degradation products by TOPKAT analyses

Model[a]	ZDV/Z7/Z9	Z1	Z2	Z3	Z4	Z5	Z6	Z8
NTP carcinogenicity call (male rat) (v3.2)	0.601205	0.635117	0.621936	0.6338	0.5827	0.614807	0.569039	0.651193
NTP carcinogenicity call (female rat) (v3.2)	0.389191	0.451652	0.425216	0.471237	0.353482	0.398239	0.380975	0.420601
NTP carcinogenicity call (male mouse) (v3.2)	0.956751	0.6046	0.609786	0.539936	0.603602	0.605863	0.900116	0.689328
NTP carcinogenicity call (female mouse) (v3.2)	**0.98775**	**0.832232**	**0.896836**	**0.595784**	**0.862657**	**0.895145**	**0.974164**	**0.872737**
FDA carcinogenicity male rat none *versus* carcinogen (v3.1)	0.223355	0.229735	0.227367	0.262078	0.226143	0.230836	0.207828	0.228379
FDA carcinogenicity female rat none *versus* carcinogen (v3.1)	0.565062	0.379458	0.436632	0.294931	0.406877	0.416319	0.434721	0.429074
FDA carcinogenicity female rat single *versus* multiple (v3.1)	0.365768	0.369808	0.319705	0.469442	0.320719	0.415096	0.266249	0.441739
FDA carcinogenicity male mouse none *versus* carcinogen (v3.1)	0.270298	0.340455	0.325645	0.401572	0.278675	0.357296	0.197168	0.348016
FDA carcinogenicity male mouse single *versus* multiple (v3.1)	0.178152	0.214562	0.211127	0.351254	0.232026	0.177657	—	0.185946
FDA carcinogenicity female mouse none *versus* carcinogen (v3.1)	**0.880708**	0.512474	0.657823	0.332135	0.611698	**0.701862**	**0.716486**	**0.707546**
FDA carcinogenicity female mouse single *versus* multiple (v3.1)	0.212682	0.255724	0.245871	0.363404	0.247947	0.227505	0.218432	0.252767
Weight of evidence carcinogenicity call (v5.1)	0.343849	0.455159	0.417765	0.551344	0.426989	0.446128	0.296666	0.444503
Ames mutagenicity (v3.1)	0.770937	0.51182	0.488866	0.663337	0.402557	0.44671	0.68296	0.534997
Developmental toxicity potential (v3.1)	0.532854	0.581491	0.575856	0.538579	0.609412	0.551531	0.591402	0.524646
Rat oral LD_{50} (v3.1) (g kg^{-1})	1.45463	1.75821	6.51255	1.79644	8.05157	7.03513	1.65473	5.69872
Rat maximum tolerated dose-feed/water (v6.1) (g kg^{-1})	0.084385	0.069803	0.198136	0.050081	0.150368	0.138981	0.06585	0.161187
Rat maximum tolerated dose-gavage (v6.1) (g kg^{-1})	**42.3725**	0.791777	0.054089	0.76531	0.216738	0.226869	15.8685	0.0965
Rat inhalational LC_{50} (v6.1) (mg m^{-3} H)	10.8997	6.47236	2.37268	4.6922	1.95652	4.233	0.976777	3.5073
Chronic LOAEL (v3.1) (g kg^{-1})	0.025337	0.014277	0.0171	0.0464	0.01105	0.009848	0.013132	0.029086
Skin irritancy none *versus* irritant (v6.1)	**0.972763**	**0.973142**	**0.973568**	**0.972897**	**0.976674**	**0.973586**	**0.976146**	**0.975179**
Skin irritancy mild *versus* moderate severe (v6.1)	—	—	—	—	0.183925	—	0.115629	0.076978
Skin sensitization none *versus* sensitizer (v6.1)	0.687369	0.660831	0.663507	0.69953	0.58999	0.633592	0.611812	0.655309
Ocular irritancy none *versus* irritant (v5.1)	**0.999058**	**0.97282**	**0.999136**	**0.998792**	**0.999228**	**0.999031**	**0.99891**	**0.999092**
Ocular irritancy mild *versus* moderate severe (v5.1)	**0.854634**	**0.853354**	**0.851304**	**0.826827**	**0.829871**	**0.853052**	**0.864532**	**0.848511**
Ocular irritancy moderate *versus* severe (v5.1)	0.621798	0.686695	0.676626	—	—	0.549875	0.688957	0.621227
Aerobic biodegradability (v6.1)	0.614863	0.63815	0.663655	0.594296	0.668784	0.675824	0.58103	0.525429
Fathead minnow LC_{50} (v3.2) (g l^{-1})	0.353352	2.09353	1.35531	2.30437	4.03792	1.26157	0.714022	0.444518
Daphnia EC_{50} (v3.1) (mg l^{-1})	10.406	4.02122	17.7645	1.58969	9.17126	10.0216	3.95292	6.60556

[a] Values in bold numbers highlight significant response and —, not predicted.

model. The results of **Z7** and **Z9** were not distinguished from the drug due to stereo-isomeric nature of these compounds. The analysis of the probability values for remaining degradation products concluded that toxicity profiles for many parameters were mostly similar to the drug. For example, mouse female NTP model highlighted carcinogenic potential of all the products. Probability values for all the degradation products for skin (none *versus* irritant) and ocular (none *versus* irritant and mild *versus* moderate) irritancy were also in the toxic zone, similar to the drug. Of course, there were exceptions, like mouse female FDA (none *versus* carcinogen) model, which showed high risk in the case of degradation products **Z5–Z9**. The value of rat maximum tolerated dose gavage (g kg^{-1}) was 42.3725 for the drug, 15.8685 for **Z6**, and for all other products. This indicated potential towards toxicity of the latter.

Conclusion

The study explored forced degradation chemistry of ZDV in both solution and solid states. The degradation products were characterized using HRMS, MS^n, NMR and IR data. Their toxicity potential was assessed using extended TOPKAT model. The drug was labile only under hydrolytic and photolytic stress

conditions. A total of nine degradation products were formed. A noteworthy observation was the generation of 3′-amino-3′-deoxythymidine (AMT, **Z2**) upon base hydrolysis and photolysis of the drug. This product is a known toxic catabolite of ZDV. *In silico* prediction also revealed toxicity potential of other degradation products. Since hydrolysis and photolysis are the two key mechanisms responsible for degradation of the drugs in the environmental matrices, the formation of more toxic degradation products **Z2** and **Z5–Z9** of ZDV under the same conditions may be a valid case to suggest their monitoring in the environment.

References

1 M. Kurmi, V. M. Golla, S. Kumar, A. Sahu and S. Singh, *RSC Adv.*, 2015, **5**, 96117–96129.
2 M. Kurmi, B. S. Kushwah, A. Sahu, M. Narayanam and S. Singh, *J. Pharm. Biomed. Anal.*, 2016, **125**, 245–259.
3 M. Kurmi, D. K. Singh, S. Tiwari, P. Sharma and S. Singh, *J. Pharm. Biomed. Anal.*, 2016, **128**, 438–446.
4 V. M. Golla, M. Kurmi, K. Shaik and S. Singh, *J. Pharm. Biomed. Anal.*, 2016, **131**, 146–155.
5 M. Kurmi, A. Sahu and S. Singh, *J. Pharm. Biomed. Anal.*, 2017, **134**, 372–384.
6 RETROVIR, http://www.accessdata.fda.gov/scripts/cder/drugsatfda/index.cfm?fuseaction=Search.DrugDetails, accessed Sep 2016.
7 A. Dunge, A. K. Chakraborti and S. Singh, *J. Pharm. Biomed. Anal.*, 2004, **35**, 965–970.
8 A. Dunge, N. Sharda, B. Singh and S. Singh, *J. Pharm. Biomed. Anal.*, 2005, **37**, 1109–1114.
9 P. S. Devrukhakar, M. S. Shankar, G. Shankar and R. Srinivas, *J. Pharm. Anal.*, 2017, DOI: 10.1016/j.jpha.2017.01.006.
10 P. Aparna, S. V. Rao, K. M. Thomas, K. Mukkanti, P. B. Gupta, K. Rangarao, G. K. Narayan, T. Sandip and K. Upendra, *Pharmazie*, 2010, **65**, 331–335.
11 J. V. dos Santos, L. A. E. B. de Carvalho and M. E. Pina, *Anal. Sci.*, 2011, **27**, 283–289.
12 D. Mandloi, P. Tripathi, P. Mohanraj, N. S. Chauhan and J. R. Patel, *J. Liq. Chromatogr. Relat. Technol.*, 2011, **34**, 601–612.
13 R. M. Kulkarni, V. S. Bhamare and B. Santhakumari, *Desalin. Water Treat.*, 2016, **57**, 24999–25010.
14 E. M. Cretton, M. Y. Xie, R. J. Bevan, N. M. Goudgaon, R. F. Schinazi and J.-P. Sommadossi, *Mol. Pharmacol.*, 1991, **39**, 258–266.
15 M. P. Stagg, E. M. Cretton, L. Kidd, R. B. Diasio and J.-P. Sommadossi, *Clin. Pharmacol. Ther.*, 1992, **51**, 668–676.
16 L. Placidi, E. M. Cretton, M. Placidi and J.-P. Sommadossi, *Clin. Pharmacol. Ther.*, 1993, **54**, 168–176.
17 AIDS by the numbers, UNAIDS 2016, http://www.unaids.org/sites/default/files/media_asset/AIDS-by-the-numbers-2016_en.pdf, accessed Sep. 2016.
18 C. Zhou, J. Chen, Q. Xie, X. Wei, Y. Zhang and Z. Fu, *Chemosphere*, 2015, **138**, 792–797.
19 S. Singh and M. Bakshi, *Pharm. Technol.*, 2000, **4**, 1–14.
20 S. Singh, M. Junwal, G. Modhe, H. Tiwari, M. Kurmi, N. Parashar and P. Sidduri, *Trends Anal. Chem.*, 2013, **49**, 71–88.
21 J. C. Dearden, *J. Comput.-Aided Mol. Des.*, 2003, **17**, 119–127.
22 K. Enslein, V. K. Gombar and B. W. Blake, *Mutat. Res.*, 1994, **305**, 47–61.
23 E. P. Acosta, L. M. Page and C. V. Fletcher, *Clin. Pharmacokinet.*, 1996, **30**, 251–262.
24 G. J. Veal and D. J. Back, *Gen. Pharmacol.*, 1995, **26**, 1469–1475.
25 *The International Pharmacopoeia*, http://apps.who.int/phint/pdf/b/Jb.6.1.435.pdf, accessed Sep. 2016.
26 Zidovudine, *United States Pharmacopeia*, USP30-NF25, 2007, p. 3489.
27 Zidovudine, *Indian Pharmacopoeia*, IP, 2010, pp. 2329–2330.
28 S. V. Zelentsov, N. V. Zelentsova, A. B. Zhezlov and A. V. Oleinik, *High Energy Chem.*, 2000, **34**, 164–171.
29 S. Brase, C. Gil, K. Knepper and V. Zimmermann, *Angew. Chem., Int. Ed.*, 2005, **44**, 5188–5240.
30 F. D. Lewis and W. H. Saunders Jr, in *Nitrenes, Interscience*, ed. W. Lwosski, New York, 1970, p. 47.
31 O. E. Edwards, in *Nitrenes, Interscience*, ed. W. Lwosski, New York, 1970, p. 225.
32 S. V. Zelentsov, N. V. Zelentsova and A. A. Shchepalov, *High Energy Chem.*, 2002, **36**, 326–332.
33 H. Peng, K. H. Dornevil, A. B. Draganov, W. Chen, C. Dai, W. H. Nelson, A. Liu and B. Wang, *Tetrahedron*, 2013, **69**, 5079–5085.

